J. Cent. South Univ. (2015) 22: 1563−1573
DOI: 10.1007/s11771-015-2673-9

Springer

Detailed string stability analysis for bi-directional optimal velocity model

ZHENG Liang(郑亮)

School of Traffic & Transportation Engineering, Central South University, Changsha 410075, China

Abstract: The class of bi-directional optimal velocity models can describe the bi-directional looking effect that usually exists in the reality and is even enhanced with the development of the connected vehicle technologies. Its combined string stability condition can be obtained through the method of the ring-road based string stability analysis. However, the partial string stability about traffic fluctuation propagated backward or forward was neglected, which will be analyzed in detail in this work by the method of transfer function and its H_∞ norm from the viewpoint of control theory. Then, through comparing the conditions of combined and partial string stabilities, their relationships can make traffic flow be divided into three distinguishable regions, displaying various combined and partial string stability performance. Finally, the numerical experiments verify the theoretical results and find that the final displaying string stability or instability performance results from the accumulated and offset effects of traffic fluctuations propagated from different directions.

Key words: traffic flow; string stability; optimal velocity model; linearized stability theory; transfer function

1 Introduction

One representative microscopic model is the car following model, especially the optimal velocity (OV) model proposed by BANDO et al [1], which is widely explored due to its simple differential equation formulation, the single-variable OV function with respect to prevailing spacing to determine desired velocity, and a rich source of dynamical behaviors. Since then, many researchers have explored the OV model from different aspects. Recent modifications to the OV model include the incorporation of driver reaction time [2−8] and the relative speed [9−10]. Moreover, what attracts our attention is that with the development of intelligent transport systems (ITS) several new variations to the OV model that incorporate spatial headways of multiple preceding vehicles appear over the last decades [11−17] and it is proved that the multiple preceding vehicles' spatial information benefits the stability of traffic flow through the analytical and numerical methods. Furthermore, in reality drivers usually not only obtain the frontal traffic stimuli but also receive the backward traffic information through rear-view mirrors and the following vehicles' honk or headlight stimuli, which can even be enhanced by the emergence of connected vehicle technologies (CVT). Therefore, highlighted by the bi-directional looking context, except some improved cellular automaton (CA) models involving the bi-directional vehicle information [18−20], many scholars are also committed to present the modified OV models based on the bi-directional looking effect [21−26] and verify that the backward traffic information contributes to the traffic flow stability through the analytical and numerical methods. Moreover, besides the stability analysis for the macroscopic traffic flow models [27−29], it should be noted that the traffic flow stability mentioned above represents the string stability analysis for the microscopic models and it is just one of the three classical stability types, which will be described in detail as the following.

Based on the general framework of the car following models proposed by WILSON [30], most car following models (including the OV models) can be cast within this framework and written as

$$\dot{v}_n = f(y_n, \Delta v_n, v_n) \tag{1}$$

where v_n is vehicle n's velocity and dot denotes the differentiation with respect to time; $y_n=x_{n+1}-x_n$ is vehicle n's distance headway with the preceding vehicle n+1; $\Delta v_n=v_{n+1}-v_n$ is the relative velocity between vehicle n and its preceding vehicle n+1; x_n denotes the position of vehicle n. Therefore, the desired state of vehicle n (i.e., the equilibrium state of vehicle n) can be described as

$$f(y^*, 0, V(y^*)) = 0 \tag{2}$$

Foundation item: Projects(51108465, 71371192) supported by the National Natural Science Foundation of China; Project(2014M552165) supported by China Postdoctoral Science Foundation; Project(20113187851460) supported by Technology Project of the Ministry of Transport of China
Received date: 2014−02−27; **Accepted date:** 2014−07−23
Corresponding author: ZHENG Liang, PhD; Tel: +86−15974236701; E-mail: zhengliang@csu.edu.cn

where y^* and $V(y^*)$ respectively indicate the vehicle n's distance headway and velocity in the equilibrium state, $V(y^*)$ is equivalent to the optimal velocity function dependant on the distance headway. On the basis of the general framework (Eq. (1)) and the equilibrium state (Eq. (2)), three kinds of stability types concerned with small amplitude perturbations, that is, platoon stability, string stability and convective stability, will be respectively defined as follows [31].

The prerequisite is as follows. Under the traffic scenario that a group of vehicles are running in an open road without the lane changing and overtaking behaviors, where each vehicle only responds to its frontal stimuli, not to its successor, and meanwhile initially keeps in the equilibrium state, that is, the velocity and distance headway of all the following vehicles are respectively $V(y^*)$ and y^* and the leading vehicle is given a fixed velocity $V(y^*)$, if the "hand of god" is applied to "kick" the first following vehicle out of the equilibrium state, the 2nd, 3rd, 4th, ⋯ , following vehicles are subsequently disturbed from equilibrium and fluctuate.

Definition 1: This group of vehicles are platoon stable at the speed $V(y^*)$ if the initial fluctuations will decay as time progresses and each individual vehicle will eventually return to its own equilibrium state. In contrast, if these fluctuations are permanent, such group of vehicles has platoon instability.

Definition 2: If the initial fluctuations will gradually dissolve when propagated upstream relative to the vehicle group, that is, the maximum deflection and duration of the fluctuation reduce when propagated upstream, the vehicle group has string stability. Otherwise, such group of vehicles are string unstable.

Definition 3: Consider that the "information" can only propagate upstream relative to the vehicles, and meanwhile the vehicles themselves are moving forward with respect to the frame of the road, therefore, whether fluctuations propagate upstream or downstream relative to the road depends on two velocities of upstream and downstream edges of one triangular "wedge" resulting from the instantaneous "kick" to the second following vehicle. This stability type called convective string stability includes convectively upstream, absolute and convectively downstream string stabilities. More details can be refered to Ref. [31].

From above three definitions, it is found that whether the fluctuation grows or decays depends on the frame of the observer, namely, the frame is defined as the individual vehicle, upstream direction relative to the vehicle group and the road for the platoon stability, string stability and convective string stability, respectively. Therefore, the platoon stable vehicle group may possess the string instability when the observing frame changes from the individual vehicle to the upstream direction relative to the vehicles. Obviously, these three definitions about the stability are beneficial to better understand the differences between each other and search the appropriate methodologies to resolve the corresponding stability conditions of Eq. (1). However, this work concentrates on the methods for the string stability condition of Eq. (1), which mainly include the ring-road based string stability analysis and H_∞ norm of transfer function from the frequency domain according to previous studies.

Since BANDO et al [1] firstly proposed the ring-road based linearized stability theory to obtain the string stability condition of the OV model [1], many scholars followed to apply this method to resolving the string stability conditions of their improved OV models [2−25]. Obviously, because the traffic fluctuation cannot escape the whole vehicular system due to the ring road setup, the string instability will result in cyclic effects (e.g., stop and go waves) in traffic flow. Meanwhile, in numerical experiments the traffic perturbation will remain bounded and not display an exponential growth due to the nonlinear terms. However, different from the ring-road based string stability analysis, there is another way to analyze the string stability of the OV models from the frequency domain. In this approach, the transfer functions can describe the transferring relationship of traffic information in car following models, and its H_∞ norm can also be employed to determine whether the traffic disturbance is amplified or decayed when propagated to one direction [32−36]. Moreover, this method was also treated as the theoretical framework of designing the advanced driver assistance (ADA) systems, such as the adaptive cruise control (ACC) [37−40], the cooperative adaptive cruise control (CACC) [41].

Obviously, this method about transfer function can describe how one vehicle's dynamics is forced by its preceding or following vehicles, which is just appropriate for the detailed analysis about the partial string stability for different parts of a vehicular system, while the ring-road based linearized stability analysis only gives the combined string stability condition. Coincidentally, the aim of this work is to investigate the partial string stability conditions of a bi-directional OV model for different directions, compare them and its combined string stability condition and then analyze the formulation mechanism of the final traffic fluctuation. Therefore, these two methods for the string stability analysis will be reviewed and then employed for one classical bi-directional OV model [21]. The remainder of this work can be organized as follows. First of all, two methods about the string stability analysis for the original OV model are reviewed. Then, two partial string

stability conditions of the bi-directional OV model are derived and then compared with combined string stability condition. After that, a series of numerical experiments are conducted to verify the obtained theoretical results. Finally, some important conclusions are drawn.

2 Two methods about string stability analysis for original OV model

The original OV model was presented by BANDO et al [1] and can be formulated as

$$\mathrm{d}v_n(t)/\mathrm{d}t=\alpha\cdot\{V[y_n(t)]-v_n(t)\} \tag{3}$$

where the car number is n (n=1, 2, ⋯, N); N is the total number of vehicles in the vehicle group; α is the sensitivity of drivers; $V[y_n(t)]$ is called the optimal velocity function (OV function) dependent on the distance headway with the nearest preceding vehicle. Obviously, the vehicle acceleration or deceleration is determined based on the difference between the optimal velocity and the immediate velocity and the driver's sensitivity.

The string stability condition of the original OV model can be obtained through the method of ring-road based linearized stability analysis [1], where a small position perturbation around the equilibrium solution ε_n can be linearized and then expanded by the Fourier modes as the following forms.

$$\varepsilon_n=\exp(\mathrm{i}\alpha_k n+zt) \tag{4}$$

where $\alpha_k=2\pi/(N\cdot k)$, k=0, 1, 2, ⋯, N−1 and z=u+iv, or

$$\varepsilon_n=\exp(\mathrm{i}kn+zt) \tag{5}$$

where $z=z(\mathrm{i}k)+z(\mathrm{i}k)+\cdots$, and k=0, 1, 2, ⋯, N−1.

Then, the string stability can be guaranteed if u<0 for Eq. (4) or z_2>0 for Eq. (5). Therefore, the string stability condition of the OV model Eq. (3) can be calculated as $2V'<\alpha$, where $V'(b)=\partial V(y)/\partial y|_{y=b}$ and b is the distance headway in the equilibrium state.

On the other hand, the string stability condition can also be obtained through the method of transfer function and its H_∞ norm [32]. In this approach, the upstream propagation of a small velocity perturbation around the equilibrium state can be described by its transfer function after the Laplace transformation and is formulated as

$$V_n(s)^{\circ}=G_n(s)\cdot V_{n+1}(s)^{\circ} \tag{6}$$

where $V_n(s)°$ and $V_{n+1}(s)°$ are respectively the velocity perturbation of vehicle n and its preceding vehicle n+1 after Laplace transformation; s=jw with the imaginary unit denoted by j and the frequency indicated by w; $G_n(s)$ is the transfer function. Moreover, whether such a small velocity fluctuation would be amplified and finally results in traffic congestion is mainly determined by the H_∞ norm of the transfer function in Eq. (6), i.e., $\|G_n(s)\|_\infty$, and if the following condition (Eq. (7)) is satisfied, we can have Eq. (8).

$$\|G_n(s)\|_\infty\le 1 \quad \text{for } n=1, 2, \cdots, N-1 \tag{7}$$

$$\|G_{k,1}\|_\infty=\|G_{k-1}\cdot G_{k-2}\cdots G_1\|_\infty\le\|G_{k-1}\|_\infty\cdot\|G_{k-2}\|_\infty\cdots\|G_1\|_\infty\le 1 \quad k=2, 3, \cdots, N \tag{8}$$

When Eq. (8) is satisfied, the velocity perturbation propagated from vehicle k ($k\ge2$) to vehicle 1 (i.e., the last following vehicle) will decay, that is also to say, the string stability of the vehicle group can be satisfied. Therefore, according to the conditions (Eqs. (7) and (8)), the string stability condition of the OV model (Eq. (3)) can also be solved out as $2\Lambda<\alpha$, where $\Lambda=\partial V(y)/\partial y|_{y=b}$.

Although the same string stability condition is reached by two different methods, their derivation processes and viewpoints are different from each other. The position perturbation around the equilibrium solution is treated as the observed quantity when applying the ring-road based linearized stability theory, which is further expanded as Fourier series, and the string stability condition can be reached only if the small disturbances with long wavelengths are mitigated. However, the method about the transfer function is focused on the transfer process of velocity fluctuation around the equilibrium solution and employing its H_∞ norm to judge whether the string stability condition can be guaranteed is from the perspective of control theory. Therefore, these two methods can also be used to analyze the stability performance of the bi-directional OV model from different viewpoints.

3 String stability conditions of bi-directional OV model

3.1 Review of bi-directional OV model and its combined string stability condition

In reality, a driver not only usually pays attention to the preceding vehicles but also perceives the states of the following vehicles through various ways, e.g., honk, headlight, rear-view mirrors or CVT, which results in the emergence of the bi-directional OV models (Fig. 1). One representative bi-directional OV model was proposed by NAKAYAMA et al [21], which in that work is called the backward looking OV (BL-OV) model and can be treated as an alternative way to mitigate the traffic congestion. Moreover, such model is formulated as

$$\mathrm{d}v_n(t)/\mathrm{d}t=\alpha\cdot\{V_{\mathrm{F}}[y_n(t)]+V_{\mathrm{B}}[y_{n-1}(t)]-v_n(t)\} \tag{9}$$

where $y_{n-1}(t)$=$x_n(t)$−$x_{n-1}(t)$ is the distance headway of the

following vehicle (n−1), $V_F(y)$ and $V_B(y)$ are the optimal velocity functions for forward and backward looking, respectively. Moreover, $V_F(y)$ is monotonically increasing function with respect to the distance to the preceding vehicle and $V_B(y)$ is monotonically decreasing function with respect to the distance to the following vehicle. In this way, the optimal velocity is not only determined by $V_F(y)$ from downstream but also by $V_B(y)$ from upstream.

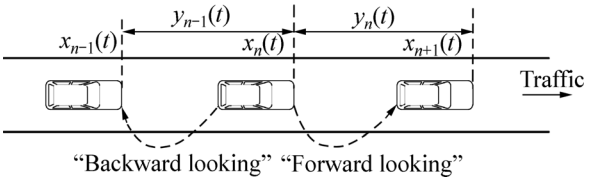

Fig. 1 Illustration of bi-directional OV model

Moreover, through the method of ring-road based string stability analysis [21], the string stability condition for such bi-directional OV model (i.e., the combined string stability condition) can be expressed as $\alpha > 2[V_F'(b)+V_B'(b)]^2/[V_F'(b)-V_B'(b)]$, where $V_F'(b) = \partial V_F(y)/\partial y|_{y=b}$ and $V_B'(b) = \partial V_B(y)/\partial y|_{y=b}$. Meanwhile, $V_F(b)+V_B(b)=V_e$, where V_e is the steady velocity in the equilibrium state. Note that $V_F'(b)$ and $V_B'(b)$ will be denoted as Λ_F and Λ_B, respectively. Therefore, the combined string stability condition can be simplified as

$$\alpha > C_L \tag{10}$$

where $C_L = 2(\Lambda_F+\Lambda_B)^2/(\Lambda_F-\Lambda_B)$.

3.2 Partial string stability conditions of bi-directional OV model

From the bi-directional OV model (Eq. (9)), the vehicular dynamical system can be written as

$$\begin{cases} \dfrac{dv_n(t)}{dt} = \alpha\cdot\{V_F[y_n(t)]+V_B[y_{n-1}(t)]-v_n(t)\} \\ \dfrac{dy_n(t)}{dt} = v_{n+1}(t)-v_n(t) \\ \dfrac{dy_{n-1}(t)}{dt} = v_n(t)-v_{n-1}(t) \end{cases} \tag{11}$$

Then, vehicular dynamical system (Eq. (11)) can be linearized around the steady state (i.e., $V_F(b)+V_B(b)=V_e$) as

$$\begin{cases} \dfrac{d\overline{v}_n(t)}{dt} = \alpha\cdot\{\Lambda_F\cdot\overline{y}_n(t)+\Lambda_B\cdot\overline{y}_{n-1}(t)-\overline{v}_n(t)\} \\ \dfrac{d\overline{y}_n(t)}{dt} = \overline{v}_{n+1}(t)-\overline{v}_n(t) \\ \dfrac{d\overline{y}_{n-1}(t)}{dt} = \overline{v}_n(t)-\overline{v}_{n-1}(t) \end{cases} \tag{12}$$

where $\overline{v}_n(t) = v_n(t)-V_e$, $\overline{y}_n(t) = y_n(t)-b$.

From the viewpoint of control theory, the dynamic system (Eq. (12)) can be rewritten as a linear time-invariant system, that is

$$\begin{bmatrix} \dot{\overline{v}}_n(t) \\ \dot{\overline{y}}_n(t) \\ \dot{\overline{y}}_{n-1}(t) \end{bmatrix} = \boldsymbol{M}\cdot\begin{bmatrix} \overline{v}_n(t) \\ \overline{y}_n(t) \\ \overline{y}_{n-1}(t) \end{bmatrix} + \begin{bmatrix} 0 \\ 1 \\ 0 \end{bmatrix}\overline{v}_{n+1}(t) + \begin{bmatrix} 0 \\ 0 \\ -1 \end{bmatrix}\overline{v}_{n-1}(t) \tag{13}$$

where $\boldsymbol{M} = \begin{bmatrix} -\alpha & \alpha\Lambda_F & \alpha\Lambda_B \\ -1 & 0 & 0 \\ 1 & 0 & 0 \end{bmatrix}$.

After Laplace transformation, the resulting dynamic system in the frequency domain becomes

$$\begin{bmatrix} \overline{V}_n(s) \\ \overline{Y}_n(s) \\ \overline{Y}_{n-1}(s) \end{bmatrix} = (s\boldsymbol{I}-\boldsymbol{M})^{-1}\begin{bmatrix} 0 \\ 1 \\ 0 \end{bmatrix}\overline{V}_{n+1}(s) + (s\boldsymbol{I}-\boldsymbol{M})^{-1}\begin{bmatrix} 0 \\ 0 \\ -1 \end{bmatrix}\overline{V}_{n-1}(s) \tag{14}$$

where $\boldsymbol{I}$ is the unit matrix, $\overline{V}_n(s) = L[\overline{v}_n(t)]$, $\overline{Y}_n(s) = L[\overline{y}_n(t)]$, $\overline{Y}_n(s) = L[\overline{y}_n(t)]$, and L denotes the Laplace transformation.

Solving system (Eq. (14)), it is obtained that vehicle n's velocity disturbance results from the velocity disturbances from its nearest preceding vehicle n+1 and following vehicle n−1, whose transferring relationship is formulated as

$$\overline{V}_n(s) = G_F(s)\cdot\overline{V}_{n+1}(s)+G_B(s)\cdot\overline{V}_{n-1}(s) \tag{15}$$

where $G_F(s) = \alpha\Lambda_F/d(s)$, $G_B(s) = -\alpha\Lambda_B/d(s)$ and $d(s) = s^2+\alpha s+\alpha(\Lambda_F-\Lambda_B)$.

Moreover, such relationship can also be depicted as the following block diagram.

As illustrated in Fig. 2, input signals of the system include velocity perturbations from the preceding vehicle (n+1) and following vehicle (n−1). The transfer functions $G_F(s)$ and $G_B(s)$ can illustrate the transfer performance of velocity disturbance when propagated backward or forward. Then, the final velocity perturbation of vehicle n is the combined results of vehicle disturbance from both directions. It should be noted that the forward looking term of Eq. (15) (i.e., the first term of the right hand side) deals with the disturbance that propagates in

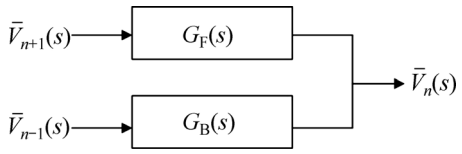

Fig. 2 Block diagram for transferring relationship of velocity disturbances

the opposite direction of traffic, that is, backward disturbance; while, the backward looking term (i.e., the second term of the right hand side) formulates the impact of forward disturbance.

3.2.1 Partial string stability analysis for backward disturbances

The magnitude of backward disturbance will not increase if the following condition is met.

$$2(\Lambda_F-\Lambda_B)-2\sqrt{\Lambda_B^2-2\Lambda_F\Lambda_B}\le\alpha \tag{16}$$

As for $G_F(s)=\alpha\Lambda_F/\mathrm{d}(s)$, when the characteristics polynomial $d(s)$ is stable, it is necessary for us to make $\|G_F(s)\|_\infty\le 1$ to guarantee that backward disturbance will not be amplified. Moreover, according to the definition of H_∞ norm of transfer function [32], the condition $\|G_F(s)\|_\infty\le 1$ can be rewritten as

$$|G_F(\mathrm{j}\omega)|=\sqrt{\frac{(\alpha\Lambda_F)^2}{(\alpha(\Lambda_F-\Lambda_B)-\omega^2)^2+\alpha^2\omega^2}}\le 1 \quad \text{for} \quad \omega\in[0,+\infty) \tag{17}$$

On one hand, it is obtained from Eq. (17) that $\omega^4+[\alpha^2-2\alpha(\Lambda_F-\Lambda_B)]\omega^2+\alpha^2(\Lambda_F-\Lambda_B)^2-(\alpha\Lambda_F)^2\ge 0$ for $\omega\in[0,\infty)$, which can also be written as $h(q)=q^2+[\alpha^2-2\alpha(\Lambda_F-\Lambda_B)]q+\alpha^2(\Lambda_F-\Lambda_B)^2-(\alpha\Lambda_F)^2\ge 0$ fo $q=\omega^2\in[0,\infty)$. Moreover, according to the features of $h(q)$, the inequality $h(q)\ge 0$ can be guaranteed if the following condition is met.

$$\begin{cases} q=\omega^2=\dfrac{2\alpha(\Lambda_F-\Lambda_B)-\alpha^2}{2}\ge 0 \\ \Delta=[\alpha^2-2\alpha(\Lambda_F-\Lambda_B)]^2-4[\alpha^2(\Lambda_F-\Lambda_B)^2-(\alpha\Lambda_F)^2]\le 0 \end{cases} \tag{18}$$

Then, from condition (Eq. (18)) we can derive the following inequality:

$$2(\Lambda_F-\Lambda_B)-2\sqrt{\Lambda_B^2-2\Lambda_F\Lambda_B}\le\alpha\le 2(\Lambda_F-\Lambda_B) \tag{19}$$

On the other hand, another stability condition can be obtained by checking the following three conditions 1) $|G_F(\mathrm{j}0)|<1$; 2) $|G_F(\mathrm{j}\infty)|=0$; 3) $\partial g(\omega)/\partial\omega=2\omega(2\omega^2-(2\alpha(\Lambda_F-\Lambda_B)-\alpha^2))\ne 0$ for $\omega\in(0,\infty)$, where $g(\omega)=(\alpha(\Lambda_F-\Lambda_B)-\omega^2)^2+\alpha^2\omega^2$. After a series of algebraic operations, the following inequality can be gotten.

$$2(\Lambda_F-\Lambda_B)\le\alpha \tag{20}$$

From Eqs. (19)−(20), it is obviously known that the backward disturbance would not be enlarged if the condition (Eq. (16)) is satisfied.

3.2.2 Partial string stability analysis for forward disturbances

Similarly, the forward disturbance will not increase if the following condition is conformed.

$$2(\Lambda_F-\Lambda_B)-2\sqrt{\Lambda_F^2-2\Lambda_F\Lambda_B}\le\alpha \tag{21}$$

Comparing Eqs. (16) and (21), their relationships between two partial string stabilities from different directions can be summarized in Table 1.

Table 1 Relationship between forward and backward string stabilities

Inequality	FS/BS	FS/NBS	NFS/BS	NFS/NBS
$\|\Lambda_B\|>\|\Lambda_F\|$	$\alpha\ge C_B$	$C_F\le\alpha<C_B$	—	$\alpha<C_F$
$\|\Lambda_B\|<\|\Lambda_F\|$	$\alpha\ge C_F$	—	$C_B\le\alpha<C_F$	$\alpha<C_B$

Note: $C_F=2(\Lambda_F-\Lambda_B)-2\sqrt{\Lambda_B^2-2\Lambda_F\Lambda_B}$ and $C_B=2(\Lambda_F-\Lambda_B)-2\sqrt{\Lambda_F^2-2\Lambda_F\Lambda_B}$.

FS and BS denote the stable transferring relationships of backward and forward disturbances, respectively; NFS and NBS indicate their unstable relationships.

3.3 Comparison of two kinds of string stability conditions

The combined string stability condition by the ring-road based linearized stability analysis has been reviewed in section 3.1, while section 3.2 has verified that the partial string stability conditions for forward and backward traffic disturbance can be reached by the method of transfer function and its H_∞ norm. In this section, a more detailed comparison is conducted to investigate the relationship between these two kinds of string stability performance. Moreover, it is set that $|\Lambda_B|<|\Lambda_F|$ because drivers are usually more sensitive to the traffic information from downstream than that from upstream.

First of all, from Eqs. (10) and (16), it is assumed that $C_F>C_L$ and after some algebra operations we can obtain the following relationship.

$$f(p)=p^3-4p^2-11p-2>0 \tag{22}$$

where $p=\Lambda_B/\Lambda_F\in(-1,\ 0)$. Then, there are three roots: p_1=−1.7198, p_2=−0.1966 and p_3=5.9164 for $f(p)=0$. Moreover, according to the characteristics of $f(p)$ (Fig. 3), it is known that $p\in(p_1,p_2)$ so as to $f(p)>0$. On the other hand, $p\in(-\infty,p_1)\cup(p_2,0)$ in order to $f(p)<0$, that is, $C_F<C_L$.

Secondly, from Eqs. (10) and (21), assume that

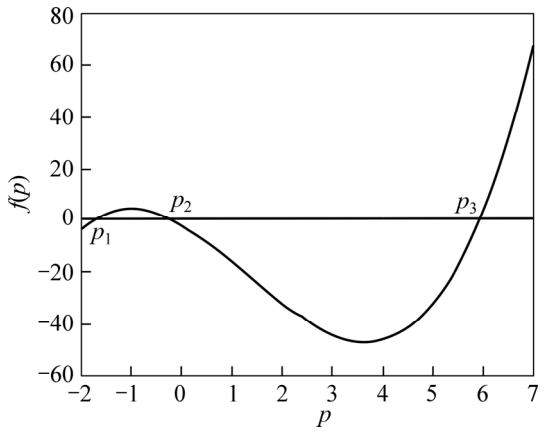

Fig. 3 Characteristics of $f(p)$

$C_B>C_L$, after some algebra operations, the following inequality can be achieved by

$$g(p)=2p^3+11p^2+4p-1>0 \tag{23}$$

where $p=\Lambda_B/\Lambda_F\in(-1, 0)$. Then, There are three roots $p'_1=-5.0876$, $p'_2=-0.5815$ and $p'_3=0.1690$ for $g(p)=0$. Furthermore, according to the characteristics of $g(p)$ (Fig. 4), $p\in(p'_1, p'_2)$ so as to $g(p)>0$. Moreover, $p\in(-\infty, p'_1)\cup(p'_2, 0)$ in order to satisfy $g(p)<0$, that is, $C_B<C_L$.

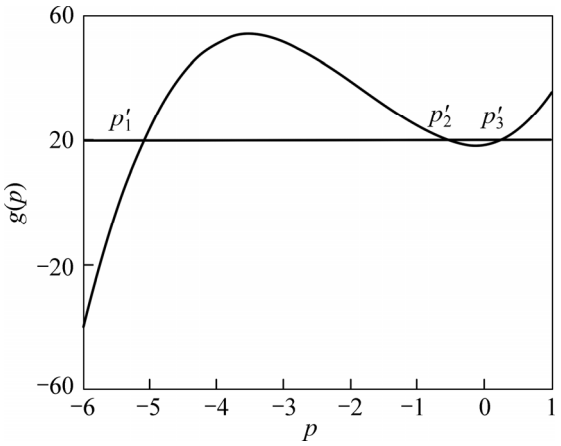

Fig. 4 Characteristics of $g(p)$

Moreover, according to the relationship of $|\Lambda_B|<|\Lambda_F|$, we have $C_F>C_B$. Therefore, based on the above derivation and analysis, their relationships can be summarized as follows.

Case 1: If $p\in(p_2, 0)$, C_L is above C_F and C_B, that is $C_L>C_F>C_B$.

Case 2: If $p\in(p_1, p_2)$ and $p\in(p'_2, 0)$ (i.e., $p\in(p'_2, p_2)$), C_L is between C_F and C_B, that is $C_F>C_L>C_B$

Case 3: If $p\in(-1, p'_2)$, C_L is below C_F and C_B, that is $C_F>C_B>C_L$.

Based on above summary and Eqs. (10), (16) and (21), the relationship between combined string stability and partial string stability from different directions is given in Table 2.

It is obviously known that if the velocity perturbations from both directions can be mitigated efficiently though their transfer functions (i.e., FS/BS), the original uniform traffic flow would be recovered finally; meanwhile, if the traffic fluctuations decay as time progresses and all vehicles finally return to their original equilibrium (i.e., CS), then the traffic disturbances transferred from upstream and downstream would vanish gradually. Therefore, three situations (i.e., FS/BS/NCS, NFS/BS/CS and NFS/NBS/CS) in Table 2 do not exist in the realistic traffic flow. Therefore, Table 2 can be modified as the following Table 3.

Table 2 Relationships between combined and partial string stability

Case	Condition	Status
1	$C_L<\alpha$	FS/BS/CS
	$C_F<\alpha<C_L$	FS/BS/NCS
	$C_B<\alpha<C_F$	NFS/BS/NCS
	$\alpha<C_B$	NFS/NBS/NCS
2	$C_F<\alpha$	FS/BS/CS
	$C_L<\alpha<C_F$	NFS/BS/CS
	$C_B<\alpha<C_L$	NFS/BS/NCS
	$\alpha<C_B$	NFS/NBS/NCS
3	$C_F<\alpha$	FS/BS/CS
	$C_B<\alpha<C_F$	NFS/BS/CS
	$C_L<\alpha<C_B$	NFS/NBS/CS
	$\alpha<C_L$	NFS/NBS/NCS

Note: CS and NCS denote the combined stability and instability of the traffic flow, respectively.

Table 3 Revised relationships between combined and partial string stabilities

Case	condition	Status
1	$C_F<\alpha$	FS/BS/CS
	$C_B<\alpha<C_F$	NFS/BS/NCS
	$\alpha<C_B$	NFS/NBS/NCS
2	$C_L<\alpha$	FS/BS/CS
	$C_B<\alpha<C_L$	NFS/BS/NCS
	$\alpha<C_B$	NFS/NBS/NCS
3	$C_L<\alpha$	FS/BS/CS
	$\alpha<C_L$	NFS/NBS/NCS

4 Numerical experiments

In the numerical experiments, N vehicles are distributed evenly in a ring road with uniform distance headway b. The length of the road is $L=N\cdot b$ and the steady-state velocity is $V_e=V_F(b)+V_B(b)$. The optimal velocity functions for forward looking and backward looking are $V_F(y)=\alpha_F\cdot[\tanh(y-y_c)+\tanh(y_c)]$ and $V_B(y)=-\alpha_B\cdot[\tanh(y-y_c)+\tanh(y_c)]$, where α_F, α_B and y_c are positive constants and $\alpha_F>\alpha_B$. The initial conditions are set as follows: the time step of simulation Δt is 0.1 s, the total number of vehicles N is 100, the steady distance headway b is 10 m and the length of the ring road L is 1000 m, $x_1(0)=b$ for $n=1$, $x_n(0)=x_{n-1}(0)+b$ for $n=2, \cdots, N$, and $v_n(0)=V_e$ for $n\neq N/2$, $v_n(0)=V_e/2$ for $n=N/2$.

4.1 Three string stability regions

According to the expressions of three neutral stability lines, i.e., C_F, C_B and C_L, traffic flow can be

divided into two regions differently by various neutral stability line, that is, traffic flow is stable above the critical line and traffic jam would not happen, while below this line traffic flow is unstable and traffic fluctuation appears. The critical point (h_c, α_c) exists for each neutral stability line under different parameters, which is indicated by the apex of each curve. Once $\alpha>\alpha_c$, the uniform state irrespective of vehicle headway is always linearly stable; while the stability would be broken for $\alpha<\alpha_c$ when headway distance is in the neighborhood of h_c.

Figure 5 illustrates three neutral stability lines

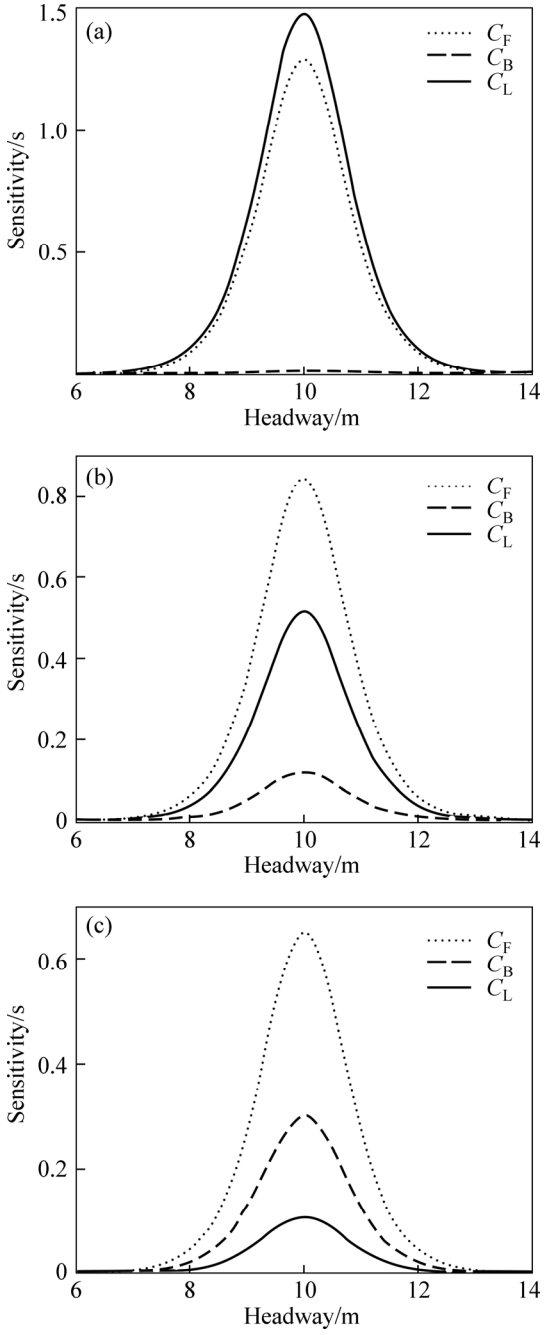

Fig. 5 Neutral stability lines in headway-sensitivity space under various situations: (a) α_B=0.1, α_F=1; (b) α_B=0.4, α_F=1; (c) α_B=0.7, α_F=1

obtained by two methods under various situations. When α_B=0.1 and α_F=1, that is, $p\in(p_2,0)$, then $C_L>C_F>C_B$ and the headway-sensitivity space is in fact divided into three parts by two neutral stability lines C_F and C_B, in which the stability performance of the traffic disturbance transferred to different direction is different from each other (Case 1 in Table 3). Similarly, when α_B=0.4 and α_F=1, i.e., $p\in(p_2', p_2)$, then $C_F>C_L>C_B$ and the headway-sensitivity space is also composed of three efficient regions separated by two neutral stability lines C_L and C_B, which is due to the relationship between the combined string stability and partial string stability (Case 2 in Table 3). However, when α_B=0.7 and α_F=1, that is, $p\in(-1, p_2')$, then $C_F>C_B>C_L$ and the headway-sensitivity space actually consists of two efficient regions divided by the neutral stability line C_L (Case 3 in Table 3).

Under the prerequisite that drivers are more sensitive to the traffic information from downstream than that from upstream, the coefficient α_F should be always larger than α_B. Therefore, in the case of $\alpha_F\leq\alpha_B$ the critical sensitivity is set as zero (Fig. 6). Figure 6(a) illustrates that when α_F is fixed, the critical sensitivity decreases with the increase of α_B, that is, the more attention to traffic information from upstream benefits the stability of backward traffic disturbance, which on the other hand would be worsened when α_B is a fixed value while α_F increases gradually (i.e., the more sensitive to the traffic information from downstream). Different from Fig. 6(a), Fig. 6(b) reflects almost the opposite relationship among α_B, α_F and α, that is, when α_F is fixed, the sensitivity of critical points increases gradually with the increase of α_B, that is, the more attention to traffic information from upstream deteriorates the stability of forward traffic disturbance, which would be improved when α_B is not changed while the critical α_F decreases gradually (i.e., the less attention to the traffic information from downstream).

Moreover, Fig. 6(c) demonstrates the ultimate critical sensitivity for such bi-directional OV model under different α_B and α_F, which is a little similar to the change trend in Fig. 6(a), that is, the critical sensitivity would increase gradually with the increase of α_F or with the decrease of α_B, which also illustrates the effect of traffic information from downstream in the stability of traffic flow outweighs that of traffic information from upstream. To sum up, by detailed comparison of three sub-figures in Fig. 6, the stable regions for forward looking, backward looking and bi-directional looking are different from each other, which reveal the difference between the transfer performance of traffic disturbance from different direction and the final stability performance of traffic flow.

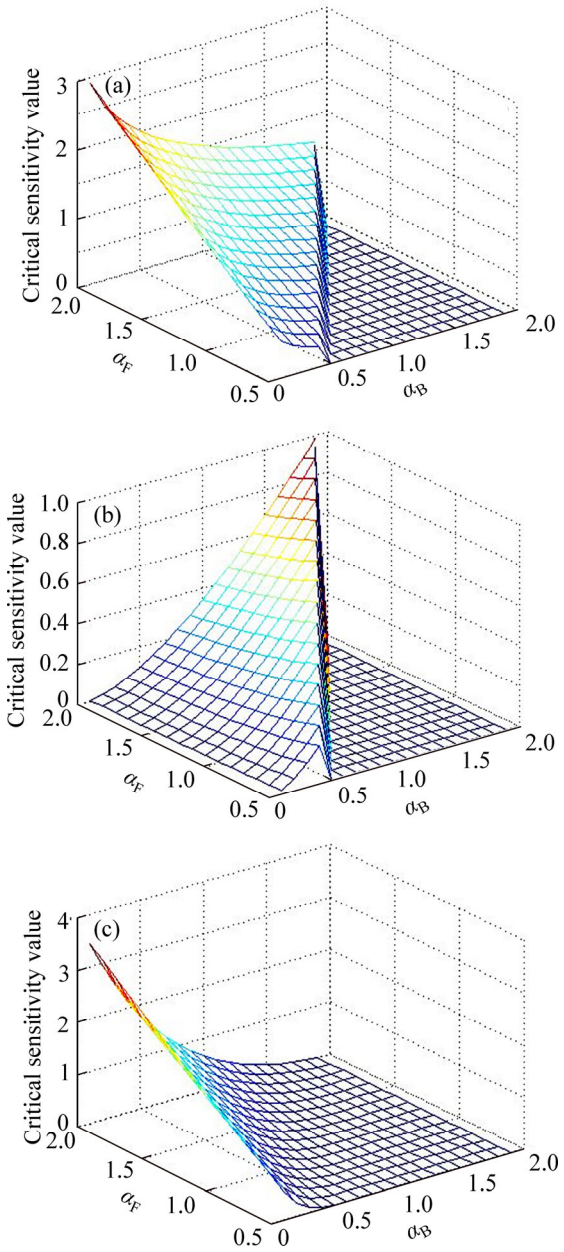

Fig. 6 Sensitivity of critical points under different situations: (a) Critical sensitivity values of C_F; (b) Critical sensitivity values of C_B; (c) Critical sensitivity values of C_L

4.2 Offset effect of velocity fluctuations from different directions

Based on the bi-directional OV model, velocity perturbation of vehicle n around the equilibrium state can not only be transferred to upstream (i.e., vehicle n−1) through $G_F(s)$, but also be transferred to downstream (i.e., vehicle n+1) through $G_B(s)$. Whether velocity perturbation of vehicle n amplifies when propagating backwards or forwards is determined by H_∞ norm of $G_F(s)$ or $G_B(s)$ respectively. Therefore, when α_F and α_B are set as 1 and 0.1 respectively (i.e., p=−0.1∈(p_2, 0)) and α is chosen as 0.5, then according to case 1 in Table 3 (or Fig. 5(a)) the transferring relationship of backward disturbance is unstable while that of forward disturbance is stable, which can also be illustrated by the responses of vehicle 49 and 51 to half reduction of vehicle 50's velocity for 10 s set in Fig. 7.

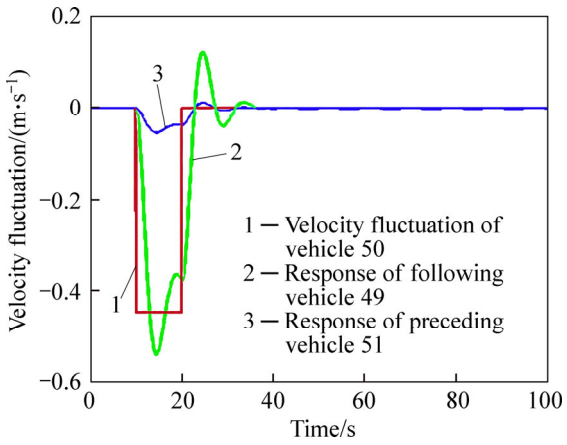

Fig. 7 Responses of two nearest vehicles to vehicle 50's velocity fluctuation (α_F=1, α_B=0.1 and α=0.5)

According to above analysis, H_∞ norm of $G_F(s)$ is larger than 1 but that of $G_B(s)$ is smaller than 1. This indicates that the backward velocity fluctuation is amplified but the forward fluctuation is not. Therefore, in the ring road, the velocity perturbations of all vehicles (Fig. 8(a)) due to the initial half velocity reduction of vehicle N/2 are transferred to upstream and cause larger and larger amplitude of velocity fluctuations (Fig. 8(b)). On the other hand, such disturbance can also be transferred to downstream; however, smaller amplitudes of velocity fluctuations (Fig. 8(c)) are yielded due to the suppression effect of $G_B(s)$. Furthermore, when comparing three subfigures in Fig. 8, it is found that ultimate velocity fluctuation is a little less serious than velocity fluctuation to upstream but much more severe than that to downstream, which implies the offset effect when the velocity fluctuation from different direction meets somewhere in the ring road.

4.3 Relationship between partial and final velocity fluctuations

According to case 2 in Table 3, when α_F and α_B are respectively set as 1 and 0.4 (i.e., $p=-0.4\in(p_2', p_2)$) and α is chosen as 0.3, then $C_B<\alpha<C_L<C_F$. In this case, H_∞ norm of $G_F(s)$ is larger than 1 while that of $G_B(s)$ is smaller than 1. Moreover, on one hand, according to the first term of the right hand side of Eq. (15), the transferring relationship about velocity fluctuation from vehicle n to its k-th following vehicle becomes

$$\overline{V}_{n-k}=G_F^{n-k}(s)\cdots G_F^{n-2}(s)\cdot G_F^{n-1}(s)\cdot\overline{V}_n,\ k\geq 1 \tag{24}$$

where $\overline{V}_{n-k}$ denotes the velocity fluctuation of the k-th following vehicle caused by vehicle n's velocity

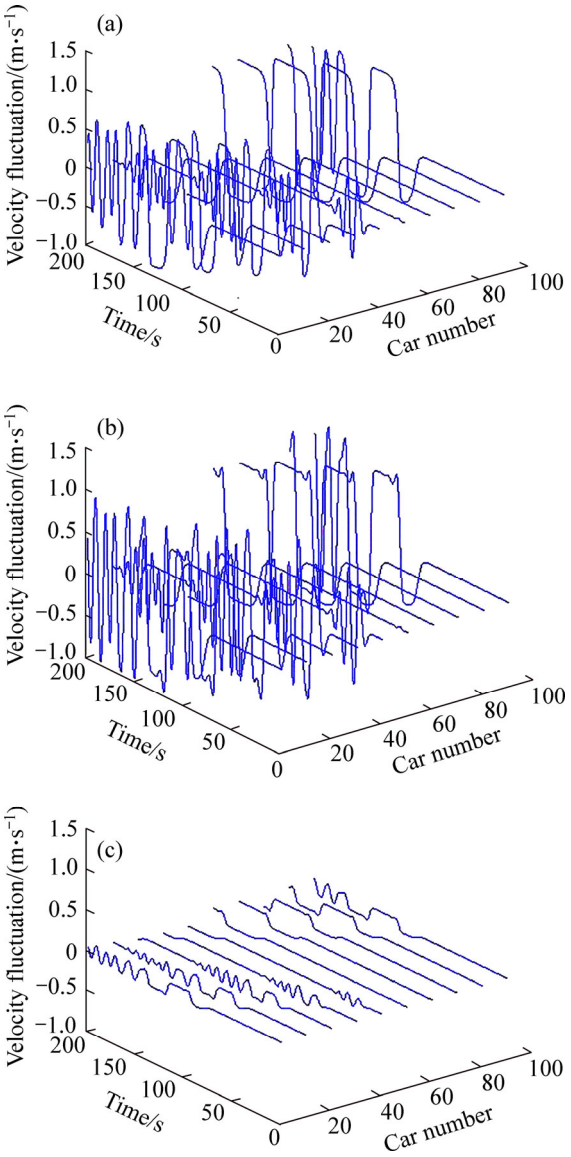

Fig. 8 Space−time evolution of velocity fluctuation (α_F=1, α_B=0.1 and α=0.5): (a) Ultimate velocity fluctuation; (b) Velocity fluctuation to upstream; (c) Velocity fluctuation to downstream

fluctuation, $G_F^{n-i}(s)$, for i=1, 2, ⋯, k is the transfer function between vehicle (n-i+1) and vehicle (n−i).

From Eq. (24), the following relationship can be easily derived.

$$\left\|\overline{V}_{n-k}/\overline{V}_n\right\|_\infty = \left\|G_F^{n-k}(s)\cdots G_F^{n-2}(s)\cdot G_F^{n-1}(s)\right\|_\infty \tag{25}$$

When $\left\|G_F^{n-i}(s)\right\|_\infty > 1$, for i=1, 2, ⋯, k, from Eq. (25) it is easily known that $\left\|\overline{V}_{n-k}/\overline{V}_n\right\|_\infty > 1$. In other words, the velocity fluctuation transferred from vehicle n to its k-th following vehicle becomes larger gradually as the k value increases (Fig. 9(a)).

On the other hand, on the basis of the second term of the right hand side of Eq. (15), the following transferring relationship about velocity fluctuation from vehicle n to its m-th preceding vehicle can be reached by

$$\overline{V}_{n+m} = G_B^{n+m}(s)\cdots G_B^{n+2}(s)\cdot G_B^{n+1}(s)\cdot\overline{V}_n,\ m\geq 1 \tag{26}$$

where $\overline{V}_{n+m}$ indicates the velocity fluctuation of the m-th preceding vehicle due to vehicle n's velocity fluctuation, $G_B^{n+j}(s)$, for j=1, 2, ⋯, m is the transfer function between vehicle (n+j−1) and vehicle (n+j).

From Eq. (26), we can gain the relationship as

$$\left\|\overline{V}_{n+m}/\overline{V}_n\right\|_\infty = \left\|G_B^{n+m}(s)\cdots G_B^{n+2}(s)\cdot G_B^{n+1}(s)\right\|_\infty \tag{27}$$

When $\left\|G_B^{n+j}(s)\right\|_\infty < 1$, for j=1, 2, ⋯, m, from Eq. (27) we have $\left\|\overline{V}_{n+m}/\overline{V}_n\right\|_\infty < 1$, that is also to say, the suppression of velocity fluctuation from vehicle n to its m-th preceding vehicle becomes more significant as the m value increases (Fig. 9(b)).

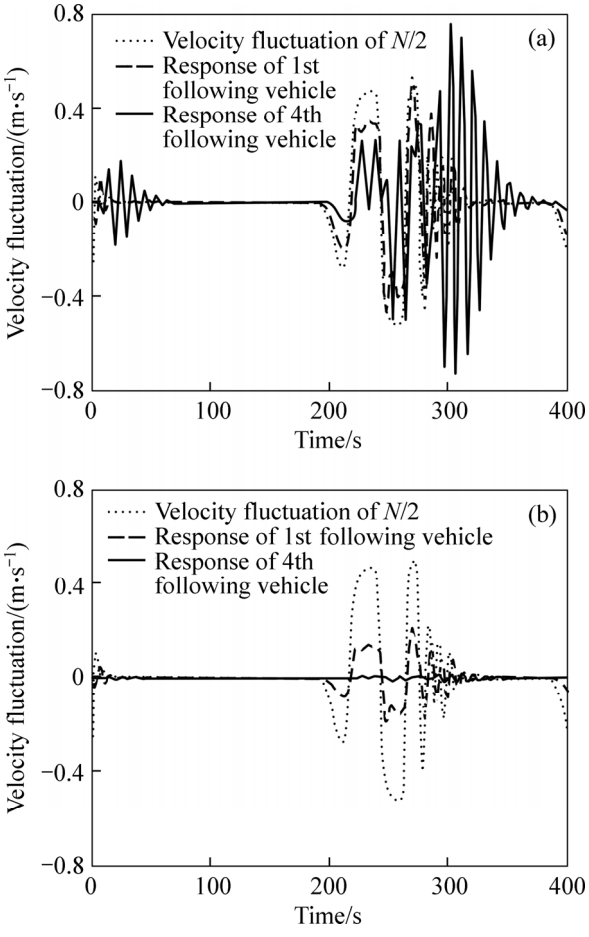

Fig. 9 Velocity fluctuation of vehicle N/2 transferred to upstream and downstream (α_F=1, α_B=0.4 and α=0.3): (a) Backward velocity fluctuation; (b) Forward velocity fluctuation

Based on above analysis about the transfer relationship of velocity fluctuation towards different directions, it is then possible to analyze the detailed cause of the combined space-time evolution of velocity fluctuation in Figs. 10(a) and (c). Obviously, because of the amplification effect of $G_F(s)$, the velocity perturbation of vehicle N/2 propagates backwards (i.e., to

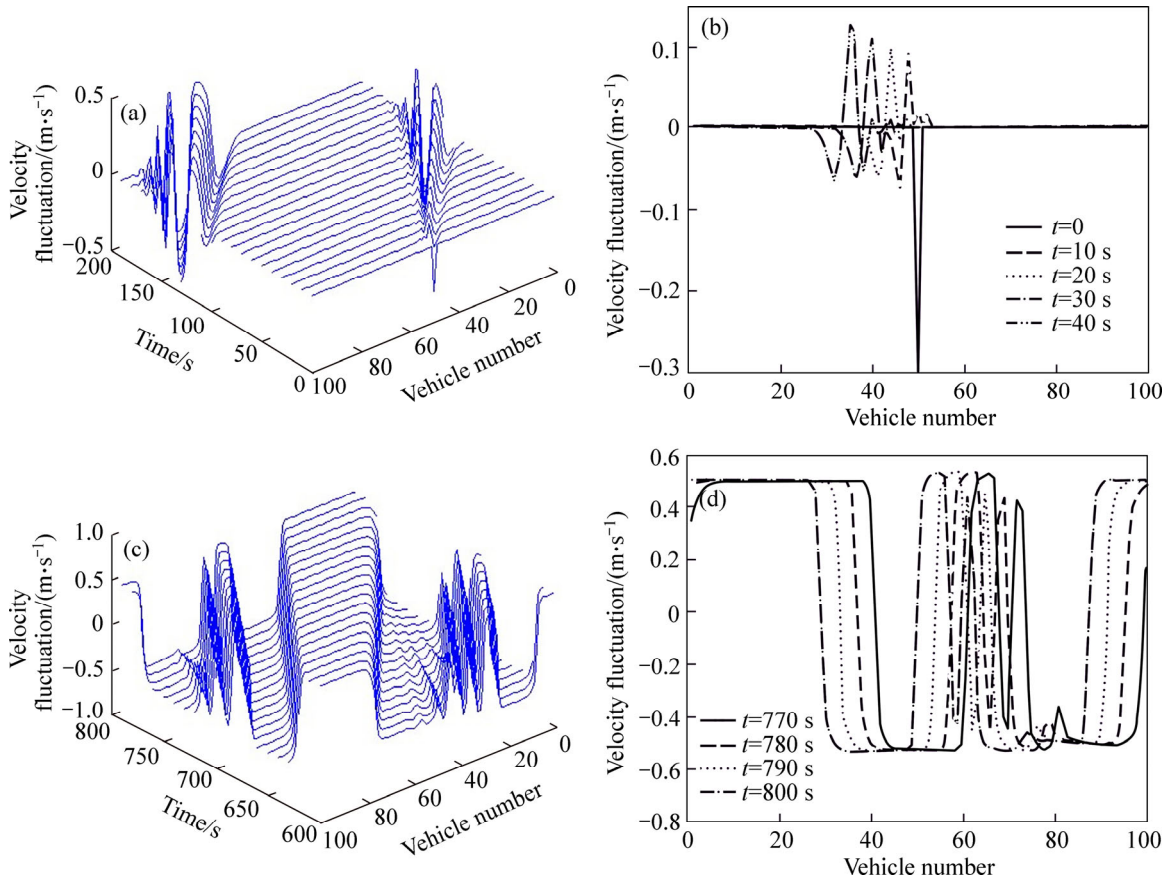

Fig. 10 Velocity fluctuation (α_F=1, α_B=0.4 and α=0.3): (a) Space−time evolution of velocity fluctuation during first 200 s; (b) Velocity fluctuation at different time; (c) Space−time evolution of velocity fluctuation during last 200 s; (d) Velocity fluctuation at different time

upstream) with increasing amplitude; while it vanishes when transferred forwards (i.e., to downstream) as a result of the suppression effect of $G_B(s)$ (Fig. 10(b)). Moreover, Figs. 10(c) and (d) illustrate that because all vehicles are running in a circular road, the growing backward velocity perturbation cannot escape from the vehicular system but rather be transferred and accumulated within the road and finally results in the periodically unstable traffic fluctuation (i.e., stop and go waves), which can also explain why the backward velocity perturbation would not always be amplified in the ring road.

5 Conclusions

1) By comparison of combined and two partial string stability conditions, the final string stability performance of traffic flow depends on the sensitivity of drivers to the forward and backward traffic stimuli.

2) The combined string instability does not necessarily indicate the partial string instability for both directions.

3) Velocity fluctuation from different directions cannot escape from the vehicular system and will meet somewhere in the ring road, which produces the offset effect and make the velocity fluctuation not always be amplified. In summary, besides of the ring-road based string stability analysis, applying the method of transfer function and its H_∞ norm to getting the partial string stability conditions can help grasp traffic flow dynamics for the bi-directional OV models in details and clearly understand how the ultimate traffic fluctuation or congestion forms.

References

[1] BANDO M, HASEBE K, NAKAYAMA A. Dynamical model of traffic congestion and numerical simulation [J]. Physical Review E, 1995, 51(2): 1035−1042.

[2] BANDO M, HASEBE K, NAKANISHI K. Analysis of optimal velocity model with explicit delay [J]. Physical Review E, 1998, 58(5): 5429−5435.

[3] DAVIS L C. Comment on “Analysis of optimal velocity model with explicit delay” [J]. Physical Review E, 2002, 66(3): 038101.

[4] DAVIS L C. Modifications of the optimal velocity traffic model to include delay due to driver reaction time [J]. Physica A, 2003, 319: 557−567.

[5] OROSZ G, WILSON R E, KRAUSKOPF B. Global bifurcation investigation of an optimal velocity traffic model with driver reaction time [J]. Physical Review E, 2004, 70: 026207.

[6] OROSZ G, KRAUSKOPF B, WILSON R E. Bifurcations and multiple traffic jams in a car-following model with reaction-time delay [J]. Physica D, 2005, 211: 277−293.

[7] YU L, LI T, SHI Z K. Density waves in a traffic flow model with reaction-time delay [J]. Physica A, 2010, 389(13): 2607−2616.

[8] CHEN J Z, SHI Z K, HU Y M. Stabilization analysis of multiple look-ahead model with driver reaction delays [J]. International Journal of Modern Physics C, 2012, 23(6): 1250048.

[9] HELBING D, TILCH B. Generalized force model of traffic dynamics [J]. Physical Review E, 1998, 58(1): 133−138.

[10] JIANG R, WU Q S, ZHU Z J. Full velocity difference model for a car-following theory [J]. Physical Review E, 2001, 64(1): 017101.

[11] LENZ H, WAGNER C K, SOLLACHER R. Multi-anticipative car-following model [J]. The European Physical Journal B, 1999, 7(2): 331−335.

[12] HAESBE K, NAHWMAA A, SUGIYAMA Y. Equivalence of linear response among extended optimal velocity models [J]. Physical Review E, 2004, 69: 017103.

[13] GE H X, DAI S Q, DONG L Y. Stabilizaiton effect of traffic flow in an extended car following model based on an intelligent transportation system application [J]. Physical Review E, 2004, 70: 066134.

[14] SHI W, CHEN N G, XUE Y. An asymptotic solvable multiple "look-ahead" model with multi-weight [J]. Conmmunications in Theoretical Physics, 2007, 48(6): 1088−1092.

[15] YU L, SHI Z K, ZHOU B C. Kink-antiKink density wave of an extended car following model in a cooperative driving system [J]. Communicaitons in Nonlinear Science and Numerical Simulation, 2008, 13(10): 2167−2176.

[16] XIE D F, GAO Z Y, ZHAO X M. Stabilizaiton of traffic flow based on the multiple information of preceding cars [J]. Communications in Computational Physics, 2008, 3: 899−912.

[17] PENG G H, SUN D H. A dynamical model of car following with the consideration of the multiple information of preceding cars [J]. Physics Letters A, 2010, 374: 1694−1698.

[18] ZHENG L, MA S F, ZHONG S Q. Analysis of honk effect on the traffic flow in a cellular automaton model [J]. Physica A, 2011, 390(6): 1072−1084.

[19] ZHENG L, MA S F, JING J, RAN B, ZHONG S Q. Incorporating backward-looking behavior into cellular automaton model [C]// 91st Annual Meeting of Transportation Research Board, Washington D. C: TRB, 2012: 12−0835.

[20] ZHENG L, ZHONG S Q, MA S F. Towards the bi-directional cellular automaton model with perception ranges [J]. Physica A, 2013, 392(14): 3028−3038.

[21] NAKAYAMA A, SUGIYAMA Y, HASEBE K. Effect of looking at the car that follows in an optimal velocity model of traffic flow [J]. Physical Review E, 2001, 65: 016112.

[22] HASEBE K, NAKAYAMA A, SUGIYAMA Y. Dynamical model of a cooperative driving system for freeway traffic [J]. Physical Review E, 2003, 68: 026102.

[23] GE H X, ZHU H B, DAI S Q. Effect of looking backward on traffic flow in a cooperative driving car following model [J]. The European Physical Journal B, 2006, 54: 503−507.

[24] SUN D H, LIAO X Y, PENG G H. Effect of looking backward on traffic flow in an extended multiple car-following model [J]. Physica A, 2011, 390(4): 631−635.

[25] YANG D, PETER J, PU Y, RAN B. Safe distance car-following model including backward-looking and its stability analysis [J]. The European Physical Journal B, 2013, 86(3): 86−92.

[26] PETER J, YANG D, RAN B, PU Y. Bi-directional control characteristics of general motors (GM) and optimal velocity car-following models: Implications for coordinated driving in connected vehicle environment [J]. Journal of the Transportation Research Board, 2013, 2381(1): 110−119.

[27] TANG T Q, LI C Y, HUANG H J, SHANG H Y. Macro modeling and analysis of traffic flow with road width [J]. Journal of Central South University of Technology, 2011, 18(5): 1757−1764.

[28] ZHANG H M. Analyses of the stability and wave properties of a new continuum traffic theory [J]. Transportation Research Part B, 1999, 33: 399−415.

[29] JIANG R, WU Q S, ZHU Z J. A new continuum model for traffic flow and numerical tests [J]. Transportation Research Part B, 2002, 36: 405−419.

[30] WILSON R E. Mechanisms for spatiotemporal pattern formation in highway traffic models [J]. Philosophical Transactions of the Royal Society Part A, 2008, 366: 2017−2032.

[31] WILSON R E, WARD J A. Car-following models: fifty years of linear stability analysis — A mathematical perspective [J]. Transportation Planning and Technology, 2011, 34(1): 3−18.

[32] KONISHI K, KOKAME H, HIRATA K. Decentralized delayed-feedback control of an optimal velocity traffic model [J]. The European Physical Journal B, 2000, 15: 715−722.

[33] ZHAO X M, GAO Z Y. Controlling traffic jams by a feedback signal [J]. The European Physical Journal B, 2005, 43(4): 565−572.

[34] ZHENG L, MA S F, ZHONG S Q. Influence of lane change on stability analysis for two-lane traffic flow [J]. Chinese Physics B, 2011, 20(8): 088701.

[35] ZHENG L, ZHONG S Q, MA S F. Controlling traffic jams on a two-lane road using delayed-feedback signals [J]. Journal of Zhejiang University: Science A, 2012, 13(8): 620−632.

[36] JIN Y F, HU H Y. Stabilization of traffic flow in optimal velocity model via delayed-feedback control [J]. Commun Nonlinear Sci Numer Simulat, 2013, 18: 1027−1034.

[37] LIANG C Y, PENG H. Optimal adaptive cruise control with guaranteed string stability [J]. Vehicle System Dynamics, 1999, 31: 313−330.

[38] LIANG C Y, PENG H. String stability analysis of adaptive cruise controlled vehicles [J]. JSME International Journal Series C, 2000, 43(3): 671−677.

[39] BOSE A, IOANNOU P. Analysis of traffic flow with mixed manual and semiautomated vehicles [J]. IEEE Transactions on Intelligent Transportation Systems, 2003, 4(4): 173−188.

[40] ZHOU J, PENG H. Range policy of adaptive cruise control vehicles for improved flow stability and string stability [J]. IEEE Transactions on Intelligent Transportation Systems, 2005, 6(2): 229−237.

[41] NAUS G J L, VUGTS R P A, PLOEG J, VAN DE MOLENGRAFT M J G, STEINBUCH M. String-stable CACC design and experimental validation: A frequency-domain approach [J]. IEEE Transactions on Vehicular Technology, 2010, 59(9): 4268−4279.

(Edited by DENG Lü-xiang)